



Computer simulation of cascade damage in α -iron with carbon in solution

Andrew F. Calder^{a,*}, David J. Bacon^a, Alexander V. Barashev^a, Yuri N. Osetsky^b

^a Department of Engineering, University of Liverpool, Brownlow Hill, Liverpool L69 3GH, UK

^b Materials Science and Technology, Oak Ridge National Laboratory, P.O. Box 2008, Oak Ridge, TN 37831-6138, USA

ARTICLE INFO

PACS:
61.80.Az
61.82.Bg

ABSTRACT

Molecular dynamics simulation method is used to investigate defect production by displacement cascades in iron with carbon (C) in solution. This is the first study of cascade damage in a metal containing interstitial solute. Iron is of particular interest because of the use of ferritic steels in plant for nuclear power generation. Cascades are simulated with energy in the range 5–20 keV in iron at either 100 or 600 K containing carbon with concentration in the range 0–1 at.%. C in solution has no discernible effect on the number of defects produced in cascades under any of the conditions simulated, nor on the clustered fraction of either self-interstitial atoms (SIAs) or vacancies. However, significant fractions of single SIAs and vacancies are trapped by C in the cascade process, irrespective of cascade energy. The fraction is independent of temperature for vacancies, but increases strongly with temperature for SIAs: this is a consequence of the higher mobility of the SIA.

© 2008 Published by Elsevier B.V.

1. Introduction

Pressure vessels of nuclear power plant have to withstand irradiation by fast neutrons and the resultant damage processes occur over wide ranges of length and time, i.e. from defect production at the atomic scale (10^{-10} m, $\sim 10^{-15}$ s) to microstructure evolution over the mesoscale (10^{-3} m, 10^9 s). Mechanisms at the finest scale are generally not amenable to direct experimental observation, and so atomic-scale computer simulation is important in predictive multiscale modelling of property changes because it can provide input to larger-scale models. Defect production in displacement cascades is an example of such simulation. Some recent reviews that describe progress in the area can be found in [1–5].

α -Iron (Fe) is the base metal for ferritic pressure vessel steels and has been the subject of many cascade damage studies. Most of these modelled pure Fe, although a few investigated the effects of chromium (Cr) or copper (Cu) in solution, which are substitutional elements in the BCC Fe lattice. The present paper considers carbon (C), which is an interstitial solute. It is known from experiment that it affects properties of intrinsic point defects [6] and microstructure development under irradiation conditions [7,8], but it is not known whether it influences defect production in the cascade itself. Possible effects could arise both in the collision phase of a cascade because of lattice distortion around C atoms, and in the thermal spike phase because of trapping of individual point defects and their clusters by solute.

Most of the MD studies of cascades mentioned above used Finnis–Sinclair-type (F–S) many-body interatomic potentials [9–11] for which the formation energy of the $\langle 110 \rangle$ dumbbell is only ~ 0.1 eV lower than that of a $\langle 111 \rangle$ crowdion. With the embedded-atom-method (EAM) potential proposed recently [12], this difference is ~ 0.5 eV and closer to the value 0.7 eV obtained by *ab initio* calculations based on the density-functional theory (DFT) [13]. Also, the $\langle 110 \rangle$ configuration is stable with respect to the $\langle 111 \rangle$ for clusters of two to four SIAs, unlike the result with the earlier potentials but in agreement with *ab initio* studies [13,14]. In a recent investigation [15], we have carried out an extensive simulation study of cascades in pure Fe using the newer interatomic potential. In the present paper, we have extended that work by modelling interstitial C in concentrations up to 1 at.% in the same model of Fe.

The paper is organised as follows. The computational method is described in Section 2. The results of the statistical analysis of point defects and their clusters created in cascades with primary knock-on atom (PKA) energy of either 5, 10 or 20 keV at either 100 or 600 K are presented in Section 3. The atomic structure of C–defect complexes is presented in Section 3.2. The conclusions are drawn in Section 4.

2. Simulation method

As noted above, the Fe–Fe potential used here and in [15] is that developed recently by Ackland et al. [12]. As in earlier cascade studies for pure Fe [10], the pair part used in the present work was modified to deal with atomic interactions at short range by using the Universal screened-Coulomb potential [16] at

* Corresponding author.

E-mail address: afcalder@liv.ac.uk (A.F. Calder).

interatomic spacing in the range $0 < x \leq x_1$, well below the perfect crystal nearest-neighbour distance $\sqrt{3}a_0/2$, where a_0 is the lattice parameter. The two potentials were joined smoothly by an exponential spline of the form

$$V(x) = \exp(B_0 + B_1x + B_2x^2 + B_3x^3) \quad (1)$$

over the range $x_1 \leq x \leq x_2$. The parameters in Eq. (1) and Eqs. (2) and (3) that follow are presented in Table 1.

Development of interatomic potentials for the Fe–C system has lagged behind those for α -Fe with substitutional solutes, and only a few Fe–C potentials have been proposed to date. We have used the simple pairwise potential of Johnson et al. [17]:

$$V(x) = J_0 + J_1x + J_2x^2 + J_3x^3. \quad (2)$$

It was fitted originally to the experimental value 0.86 eV for the migration energy of a C interstitial [18] and a vacancy–C binding energy of 0.41 eV [19]; other properties obtained with it are discussed in [20]. In summary, it gives the octahedral site as the most stable one for the C interstitial and the tetrahedral site as the saddle-point for C jump from one octahedral site to another, which is consistent with experiment [21] and DFT calculations [22]. The relaxation of Fe atoms neighbouring a C atom and the binding energy of a vacancy–C pair (0.51 eV) are in good agreement with values found by recent *ab initio* calculations [22]. However, an unresolved problem using any of the potentials in the literature concerns the interaction energy of C atom with SIAs. For example, DFT calculations show repulsion between a C atom and a single SIA in $\langle 110 \rangle$ dumbbell configuration, with a binding energy of -0.19 eV for the largest model considered [22]. In contrast, experiments offer evidence that SIAs are immobilised by C atoms and the recovery stage I_E in Fe–C solutions is attributed to dissociation of SIA–C complexes, the binding energy of which is estimated to be ~ 0.1 eV [6,23]. The potential set used here gives 0.57 eV, a value similar to that given by all Fe–C potentials developed to date. Clearly, there is an anomaly between atomic-level simulation, *ab initio* calculation and experiment that is not yet resolved, and so it is best to consider the system studied here as a model for an interstitial solute in Fe with some properties close to those of C. This potential was not developed to deal with atomic interactions at small distances and so we joined it smoothly to the C–Fe Universal potential [16] by an exponential spline (Eq. (1)) over the range $x_1 \leq x \leq x_2$.

Since C atoms can collide with each other in the cascade process even in dilute solution, it was necessary to employ a C–C potential. We could not find a suitable one in the literature and so used a simple repulsive pair C–C potential consisting of the Universal function for C–C for $0 < x \leq x_1$, a spline as in Eq. (1) for $x_1 \leq x \leq x_2$ and another

$$V(x) = A(x - x_3)^2 / (x_2 - x_3)^2 \quad (3)$$

to take it smoothly to zero at $x_3 > x_2$.

Table 1

Parameters used for the pairwise interatomic potential functions given by Eqs. (1)–(3) in the text

Fe–C					
x_1	x_2	B_0	B_1	B_2	B_3
0.5	1.5	8.522916032	-5.139071123	0.733313284	-0.927009140
C–C					
x_1	x_2	B_0	B_1	B_2	B_3
1.5	2.5	9.069913005	-9.581178982	4.588854745	-0.986031720
	x_3	A			
	2.9	0.2			

Energy unit is eV when distances x, x_1, x_2, x_3 are in Å.

The MD box was a cube with $\langle 100 \rangle$ axes and periodic boundary conditions. It was maintained at constant volume with a_0 set to the zero-pressure value for the chosen C composition and temperature, which was either 100 or 600 K. C atoms were introduced into octahedral interstitial sites chosen on a constrained random basis, i.e. random but constrained so that C atoms were at least $3a_0$ apart. The initial intention was to consider C concentration, c , across the range $0(0.1)1$ at.%, i.e. 0 to 1 in 0.1 intervals, but as results emerged, it became clear that it was unnecessary to treat all 66 conditions, i.e. two temperatures, three energies and eleven compositions, and so a more restricted set was modelled (see Section 3). In relation to the solubility of carbon in α -Fe, the maximum c considered is large. This was to ensure that any effects barely discernible at c less than about 0.1 at.% would be identified in the higher part of the concentration range.

The crystals were equilibrated prior to initiation of the Fe PKA, which had a kinetic energy E_p of 5, 10 or 20 keV. To minimise channelling, the PKA was initiated in different $\langle 135 \rangle$ and $\langle 123 \rangle$ directions for each event, and different atoms in the crystal were used at different equilibration times to provide a unique starting condition for each of the 30 cascades per condition. The MD box contained 250000, 500094 and 2000000 Fe atoms for $E_p = 5, 10$ and 20 keV, respectively. This was sufficiently large to limit the increase in lattice temperature once the PKA energy was dissipated to less than 80 K for 5 and 10 keV and less than 30 K for 20 keV.

In the ballistic phase of a cascade, a few atoms move with high velocity and the accuracy of the MD simulation is governed by integration of their equations of motion. We used a technique in which a variable time-step inversely proportional to the speed of the fastest atom was used in crystal regions containing these ‘hot’ atoms and, to avoid computational inefficiency, atoms outside these regions had longer time-steps. Separate integration was continued up to the moment when the whole volume was assigned as hot and the equations of motion of all atoms were then integrated with the same time-step, still inversely proportional to the speed of the fastest atom. (Details are in [15].)

3. Results and discussion

3.1. Number of point defects

The number, N_F , of either vacancies or SIAs produced on average per cascade under all conditions studied is presented in Fig. 1. The data points are the means for the 30 cascades simulated at each condition and the bars on each point show the standard error. The N_F value for pure Fe at 600 K is 11.1, 18.2 and 37.8 for $E_p = 5, 10$ and 20 keV, respectively, compared with 50, 100 and 200 given by the NRT standard equation with an average threshold displacement energy of 40 eV [24]. The efficiency of defect production in cascades simulated with the newer potential for Fe is lower than that predicted with the older F–S model, for which the corresponding mean numbers are 19.1, 30.5 and 55.8 [15].

The first simulations in the series were undertaken for $E_p = 5$ keV and $c = 0(0.1)1$ at.% at $T = 600$ K, and they provide the most comprehensive data set in Fig. 1. N_F is seen to decrease from 10.6 to 8.9 as c increases to 0.4 at.% and then increase to 10.5 when $c = 1\%$. Based on the standard error bars for 30 cascades per condition, the minimum at $c = 0.4\%$ may be significant. Note, however, that the spread of individual N_F values is large: the largest and smallest values were 5 and 21 for pure Fe compared with 4 and 19 for the 0.4% alloy.

In light of these results, it was decided to see if small concentrations of C had any effect on N_F for 20 keV cascades and, if not, only model the extreme values of c (0 and 1 at.%) for the other E_p and T conditions. The results for N_F are plotted in Fig. 1. From the

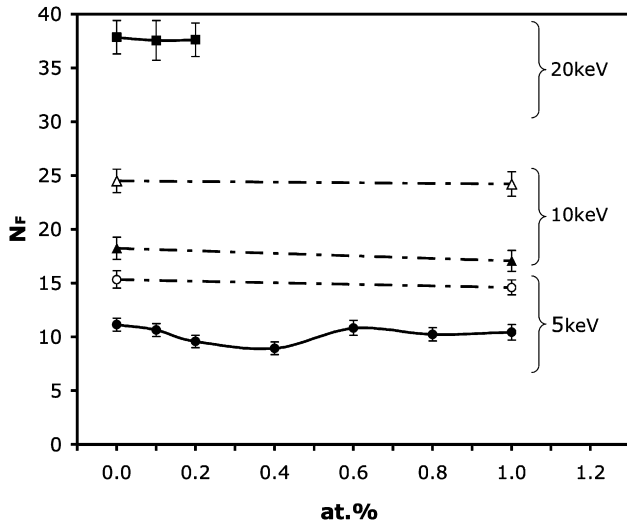


Fig. 1. Number, N_F , of vacancies and SIAs versus carbon concentration, c at.%, for all conditions studied. Data points are mean values for 30 cascades and bars are the standard error. Solid symbols: 600 K; open symbols: 100 K. In this and subsequent figures, lines between data points are drawn to guide the eye and are not fits to particular models for the data.

data for 20 keV cascades, it is seen that the effect of carbon solute on N_F for small values of c found at 5 keV is not reproduced at the higher energy. Furthermore, the N_F data when $c = 0$ or 1 at.% for the other conditions shows that interstitial C in solution has no discernible effect on the number of defects produced in cascades at either 600 or 100 K. This can be interpreted as an effect arising from the thermal spike phase of a cascade, in which recombination between displaced atoms and vacant sites is unaffected by the relatively high C–vacancy and C–SIA binding energy values of 0.51 and 0.57 eV, respectively. Note that a similar null effect was found in previous simulations of cascades in metals containing the substitutional solutes Cr and Cu, where the binding energy of solutes with intrinsic defects tends to be smaller, e.g. [25–28]. The exception is Fe–He, where vacancy trapping by He atoms was found to enhance the production of defects in simulated cascades [29].

3.2. Clustering of defects and carbon

Previous simulation studies have established that a significant fraction of point defects cluster with their own kind during the cascade process (e.g. [4]). In Fe, the fraction of defects in clusters tends to be higher for SIAs than vacancies. SIA clusters are generally in close-packed arrangements of $\langle 110 \rangle$ dumbbells for two to four defects and $\langle 111 \rangle$ crowdions for larger size, whereas vacancies tend to form looser, 3-D complexes. In this work as in previous publications, a pair of defects is considered to be a cluster if the distance between their centres of gravity is smaller than $1.05a_0$. The mean fraction of defects that are *not* in clusters is plotted as a function of C concentration in Fig. 2 for 5 keV cascades in Fe–C at 600 K. This fraction of N_F that is single is the complement of the clustered fraction. The difference between vacancies and SIAs is independent of c . Interestingly, the minimum in N_F at 0.4% in Fig. 1 is reflected in a maximum in the fraction of single defects in Fig. 2, suggesting a possible inhibition of clustering at this composition. However, the clustered fraction of vacancies and SIAs for the other conditions simulated showed no significant effect of carbon in general. This is clear from the data for the mean fraction of clustered defects for all the simulations of two energies and two temperatures with $c = 0.2$ and 1 at.% presented in Table 2.

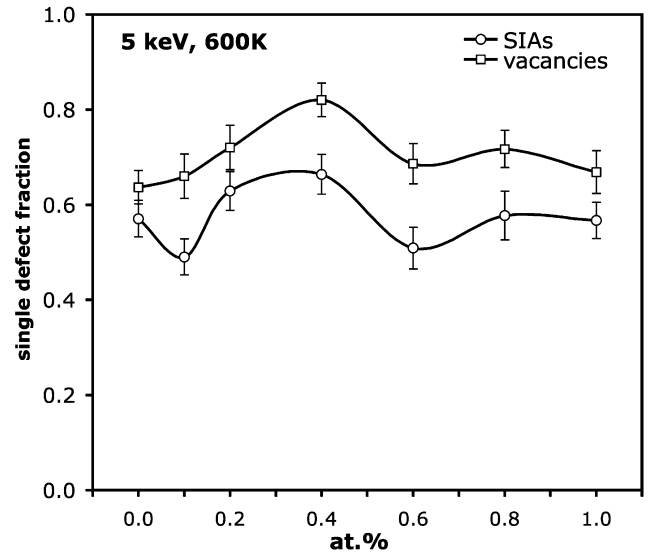


Fig. 2. Fraction of vacancies and SIAs created as single, unclustered point defects by 5 keV cascades in Fe at 600 K as a function of C concentration.

The numbers in parentheses in the table are for pure Fe. The clustered fraction of SIAs increases with increasing E_p and T in pure Fe but there is no clear trend for vacancies. The presence of carbon in solution is seen to have little effect on the fractions. It is worth noting that N_F with the interatomic potential used here is smaller than that found with the earlier F–S potential (see Section 3.1). Furthermore, the clustered fraction is smaller for SIAs and larger for vacancies. Thus, the average number of clustered defects per cascade is much smaller (by about 50%) for SIAs but about the same for vacancies [15].

Despite the absence of effects of carbon on the production and clustering of defects in the cascade process, it is of interest to see if there is evidence that single point defects are trapped at C interstitials by the end of the thermal spike phase. To do this, octahedral interstitial sites within the range $0.73a_0$ of the lattice site of every single vacancy and $\langle 110 \rangle$ dumbbell SIA in the cascade debris were searched to detect the presence of C. With the potential set used here, the vacancy–C binding energy is 0.51 eV for the six sites of nearest-neighbour coordination at $0.5a_0$ and negative for the other 12 sites within the range [20]. The SIA–C binding energy is 0.57 eV for the two nearest sites at $0.5a_0$, 0.19 eV for two of the second-neighbour sites at $0.707a_0$ and 0.33 eV for eight other such sites. The mean value of the fraction of the single point defects that have at least one C atom in a nearest-neighbour site at the end of the cascade is plotted as a function of c in Fig. 3 for 5 keV cascades in Fe at

Table 2

Mean value of the fraction of N_F created in clusters of two or more and the fraction of single defects with a C atom in a nearest-neighbour octahedral site for cascades in either Fe–0.2% C or Fe–1 at.% C

c (at.%)	E_p (keV)	T (K)	Fraction of clustered SIAs	Fraction of single SIAs with C	Fraction of clustered vacancies	Fraction of single vacancies with C
1	5	100	0.26 (0.26)	0.16	0.41 (0.41)	0.27
		600	0.43 (0.46)	0.69	0.33 (0.39)	0.35
	10	100	0.33 (0.30)	0.20	0.32 (0.34)	0.31
		600	0.43 (0.47)	0.56	0.27 (0.21)	0.37
0.2	5	600	0.37 (0.46)	0.33	0.28 (0.39)	0.11
	20	600	0.63 (0.59)	0.17	0.45 (0.41)	0.08

Numbers in parentheses are for pure Fe.

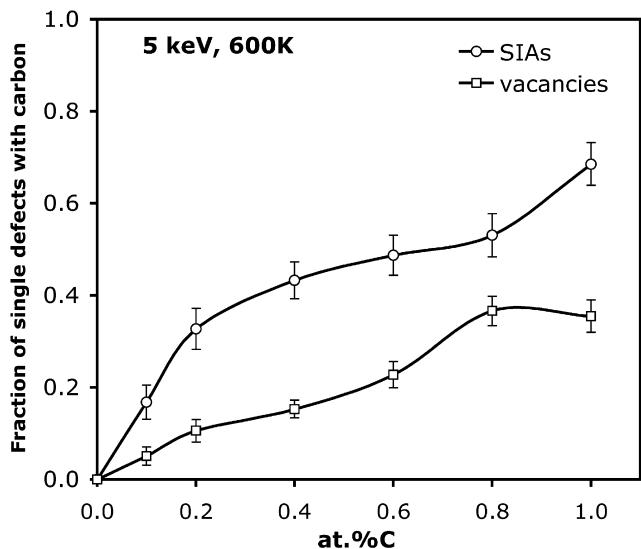


Fig. 3. Fraction of single vacancies and SIAs created with at least one carbon atom in a nearest-neighbour octahedral site by 5 keV cascades in Fe at 600 K as a function of C concentration.

600 K. If carbon solute atoms were inserted randomly to a concentration c (in at.%) in iron containing single vacancies and SIAs, the fraction of these defects that would have a C atom in neighbouring site with positive binding energy would be $6c/100$ for vacancies and $12c/100$ for SIAs. Within the statistical error, the fraction does increase approximately linearly with c for vacancies, but the gradient is nearer to 0.4 than 0.06, hence about seven times higher. The statistics for SIAs show that their association with C solute is even stronger. These results show that binding energy ~ 0.5 eV is sufficient to cause a substantial fraction of the intrinsic single point defects to form solute-defect pairs during the cascade process. For the 5 keV cascades discussed here, the mean number of single vacancies and SIAs that are not paired with C falls from approximately 7 to 4 and 5 to 1, respectively, as c increases from 0 to 1 at.%. The strong effect for SIAs is believed to arise from trapping by C during the thermal spike phase.

Data showing how the fraction of single point defects created with at least one nearest-neighbour C atom varies with E_p and T for the 0.2 at.%C and 1 at.%C alloys is presented in Table 2. For $c = 1$ at.% the data for 5 and 10 keV are similar. The fractions of SIAs and vacancies in pairs with C are around 0.2–0.3 at both energies at 100 K, and the fraction for vacancies at 600 K is only slightly higher. The fraction for SIAs paired with C is raised to around 0.6 at 600 K, however. The fractions for $c = 0.2$ at.% are slightly smaller at 20 keV than 5 keV, but again the fraction of SIAs paired with C is higher than the fraction for vacancies. The enhancement of SIA trapping at C as the thermal spike decays is believed to arise from the relatively high mobility of SIAs, for the migration energy of the $\langle 110 \rangle$ dumbbell with the interatomic potential used is 0.34 eV compared with 0.63 eV for the vacancy. The effect is particularly strong at 600 K, where the lifetime of the thermal spike over which an SIA can jump is longer.

The activation energy of solute migration in the model used is 0.82 eV, which is close to the experimental value for C in α -Fe (see data in [20]), and the nature of the C–C potential employed is repulsive (Eq. (3)), so no solute clustering was either expected or found in the cascade simulations.

4. Conclusions

An MD model for interstitial solute atoms of low mass occupying octahedral sites in a BCC metal, representing C in α -Fe, has

been used to investigate the possible influence of this solute on the formation of defects in displacement cascades. (The PKA used to create a cascade was Fe in all cases. The effect on cascade damage in pure Fe of changing the PKA to lighter (C) or heavier (Bi) atoms has been presented elsewhere [30].) Thirty cascades have been simulated for each combination of temperature, T , solute concentration, c , and cascade energy, E_p , in order to generate meaningful statistics, and the model size in each case was large enough to avoid boundary and heating effects that may influence the results of cascade simulation. Artificially large values of c (up to 1 at.%) have been used in order to ensure detection of any effects of interstitial solute on cascade damage. The conclusions drawn are as follows:

1. With the newer interatomic potential used for Fe–Fe interactions [12], the number, N_F , of vacancies or SIAs created by cascades in pure Fe is lower by about 40% than that found in simulations based on an earlier potential [11].
2. Over the composition range considered, $c = 0$ –1 at.%, C in solution has no discernible effect on the number of defects produced at either 100 or 600 K in cascades with energy in the range 5–20 keV. This is similar to the null effect found in previous simulations of cascades in metals containing substitutional solute.
3. Previous MD modelling has shown that a sizeable fraction of SIAs and vacancies cluster with their own kind in the cascade process. The present work shows that C has no significant effect on the clustered fraction of either SIAs or vacancies under any of the c , T and E_p conditions simulated.
4. Interstitial solute does have an influence on the entrapment of single SIAs and vacancies in the cascade process. It is found that a much larger proportion of these defects has a C atom in a near-neighbour octahedral site than would be the case with random occupancy. The proportion is insensitive to E_p . It is also independent of T for vacancies, but increases strongly for SIAs as T increases from 100 to 600 K. This is a consequence of the lower migration energy of the $\langle 110 \rangle$ dumbbell SIA compared with a vacancy.

Acknowledgments

The research was supported by grant GR/S81162/01 from the UK Engineering and Physical Sciences Research Council; Grant F160-CT-2003-508840 ('PERFECT') under programme EURATOM FP-6 of the European Commission; and partly by the Division of Materials Sciences and Engineering and the Office of Fusion Energy Sciences, US Department of Energy, under Contract DE-AC05-00OR22725 with UT-Battelle, LLC.

References

- [1] D.J. Bacon, A.F. Calder, F. Gao, J. Nucl. Mater. 251 (1997) 1.
- [2] D.J. Bacon, T. Diaz de la Rubia, J. Nucl. Mater. 216 (1994) 275.
- [3] D.J. Bacon, F. Gao, Y.N. Osetsky, J. Nucl. Mater. 276 (2000) 1.
- [4] D.J. Bacon, Yu. N. Osetsky, R. Stoller, R.E. Voskoboinikov, J. Nucl. Mater. 323 (2003) 152.
- [5] L. Malerba, J. Nucl. Mater. 351 (2006) 28.
- [6] A. Vehanen, P. Hautajarvi, J. Johansson, J. Yli-Kaupilla, P. Moser, Phys. Rev. B 25 (1982) 762.
- [7] E.A. Little, J. Nucl. Mater. 87 (1979) 11.
- [8] E.A. Little, D.A. Stow, J. Nucl. Mater. 87 (1979) 25.
- [9] M.W. Finnis, J.E. Sinclair, Philos. Mag. A 50 (1984) 45.
- [10] A.F. Calder, D.J. Bacon, J. Nucl. Mater. 207 (1993) 25.
- [11] G.J. Ackland, D.J. Bacon, A.F. Calder, T. Harry, Philos. Mag. A 75 (1997) 713.
- [12] G.J. Ackland, M.I. Mendeleev, D.J. Srolovitz, S. Han, A.V. Barashev, J. Phys. Condens. Matter 16 (2004) S2629.
- [13] F. Willaime, C.C. Fu, M.C. Marinica, J. Dalla Torre, Nucl. Instrum. and Meth. B 228 (2005) 92.
- [14] C.C. Fu, F. Willaime, P. Ordejon, Phys. Rev. Lett. 92 (2004) 175503.

- [15] R.E. Voskoboinikov, Yu.N. Osetsky, D.J. Bacon, *J. Nucl. Mater.* 377 (2008) 385.
- [16] J.P. Biersack, J.F. Ziegler, *Nucl. Instrum. and Meth.* 194 (1982) 93.
- [17] R.A. Johnson, G.J. Dienes, A.C. Damask, *Acta Metall.* 12 (1964) 1215.
- [18] C.A. Wert, *Phys. Rev.* 79 (1950) 601.
- [19] R.A. Arndt, A.C. Damask, *Acta Metall.* 12 (1964) 341.
- [20] K. Tapasa, A.V. Barashev, D.J. Bacon, Yu.N. Osetsky, *Acta Mater.* 55 (2007) 1.
- [21] G.K. Williamson, R.E. Smallmann, *Acta Crystallogr.* 6 (1953) 361.
- [22] C. Domain, C.S. Becquart, J. Foct, *Phys. Rev. B* 69 (2004) 144112.
- [23] S. Takaki, J. Fuss, H. Kugler, U. Dedek, H. Schults, *Radiat. Eff.* 79 (1983) 87.
- [24] M.J. Norgett, M.T. Robinson, I.M. Torrens, *Nucl. Eng. Des.* 33 (1975) 50.
- [25] A.F. Calder, D.J. Bacon, *Mater. Res. Soc. Symp. Proc.* 439 (1997) 521.
- [26] C.S. Becquart, C. Domain, J.C. van Duysen, J.M. Raulot, *J. Nucl. Mater.* 294 (2001) 274.
- [27] D.A. Terentyev, L. Malerba, R. Chakarova, K. Nordlund, P. Olsson, M. Rieth, J. Wallenius, *J. Nucl. Mater.* 349 (2006) 119.
- [28] J.-H. Shim, H.-J. Lee, B.D. Wirth, *J. Nucl. Mater.* 351 (2006) 56.
- [29] L. Yang, X.T. Zu, H.Y. Xiao, F. Gao, H.L. Heinisch, R.J. Kurtz, K.Z. Liu, *Appl. Phys. Lett.* 88 (2006) 091915.
- [30] A.F. Calder, D.J. Bacon, A.V. Barashev, Yu.N. Osetsky, *Philos. Mag. Lett.* 88 (2008) 1.